Targeting RPL39 and MLF2 reduces tumor initiation and metastasis in breast cancer by inhibiting nitric oxide synthase signaling

Bhuvanesh Dave[a,1], Sergio Granados-Principal[a,1], Rui Zhu[b], Stephen Benz[c], Shahrooz Rabizadeh[d], Patrick Soon-Shiong[d], Ke-Da Yu[e], Zhimin Shao[e], Xiaoxian Li[f], Michael Gilcrease[f], Zhao Lai[g], Yidong Chen[g,h], Tim H.-M. Huang[i,j], Haifa Shen[k], Xuewu Liu[k], Mauro Ferrari[k], Ming Zhan[b], Stephen T. C. Wong[a,b], Muthiah Kumaraswami[l,m], Vivek Mittal[n], Xi Chen[n], Steven S. Gross[n], and Jenny C. Chang[a,2]

[a]Houston Methodist Cancer Center, Houston, TX 77030; [b]Department of Systems Medicine and Bioengineering, Houston Methodist Research Institute, Houston, TX 77030; [c]Five3 Genomics, Santa Cruz, CA 95060; [d]Chan Soon-Shiong Institute for Advanced Health, Culver City, CA 90232; [e]Department of Breast Surgery, Shanghai Cancer Center and Cancer Institute of Fudan University, Shanghai 200032, China; [f]Univestity of Texas MD Anderson Cancer Center, Houston, TX 77030; [g]Greehey Children's Cancer Research Institute, [h]Department of Epidemiology and Biostatistics, [i]Department of Molecular Medicine, and [j]Cancer Therapy and Research Center, University of Texas Health Science Center at San Antonio, San Antonio, TX 78229; [k]Department of NanoMedicine, Houston Methodist Research Institute, Houston, TX 77030; [l]Center for Molecular and Translational Human Infectious Diseases Research, Houston Methodist Research Institute and [m]Department of Pathology and Genomic Medicine, Houston Methodist Hospital System, Houston, TX 77030; and [n]Weill Cornell Medical College, New York, NY 10065

Edited* by Robert A. Weinberg, Whitehead Institute for Biomedical Research, Department of Biology, Massachusetts Institute of Technology, and Ludwig MIT Center for Molecular Oncology, Cambridge, MA, and approved April 17, 2014 (received for review November 11, 2013)

We previously described a gene signature for breast cancer stem cells (BCSCs) derived from patient biopsies. Selective shRNA knockdown identified ribosomal protein L39 (RPL39) and myeloid leukemia factor 2 (MLF2) as the top candidates that affect BCSC self-renewal. Knockdown of RPL39 and MLF2 by specific siRNA nanoparticles in patient-derived and human cancer xenografts reduced tumor volume and lung metastases with a concomitant decrease in BCSCs. RNA deep sequencing identified damaging mutations in both genes. These mutations were confirmed in patient lung metastases ($n = 53$) and were statistically associated with shorter median time to pulmonary metastasis. Both genes affect the nitric oxide synthase pathway and are altered by hypoxia. These findings support that extensive tumor heterogeneity exists within primary cancers; distinct subpopulations associated with stem-like properties have increased metastatic potential.

Large-scale sequencing analyses of solid cancers have identified extensive tumor heterogeneity within individual primary cancers (1). Recent studies indicate that such tumoral heterogeneity is associated with heterogeneous protein function, which fosters tumor adaptation, treatment resistance, and failure through Darwinian selection (2–4). Cancer stem cells are a subpopulation of cells within the primary tumor responsible for tumor initiation and metastases (5–9). Three groups have recently independently provided functional evidence for the presence of cancer stem cells by lineage-tracing experiments (10–12). These observations suggest that these subpopulations of cancer stem cells (CSCs) within the bulk primary tumor are resistant to conventional therapies through different adaptive mechanisms with the potential for self-renewal and metastases (7, 13, 14). However, few studies have determined the genetic profile of the cells that escape the primary cancer and evolve in distant metastatic sites (1). Additionally, no large-scale sequencing studies of metastases have been conducted because the majority of patients are treated with systemic therapies and not surgery.

Tumor clonal heterogeneity within a primary tumor may in part be explained by hypoxic regions within the bulk tumor that have been correlated with invasiveness, therapeutic resistance, and metastasis (15–18). Cancer stem cells have been found to reside near hypoxic regions in some solid cancers (19–21). We have previously published a 477-gene tumorigenic signature by isolating breast cancer stem cells (BCSCs) derived from patient biopsies (22). Here, we have identified two previously unidentified cancer genes, ribosomal protein L39 (RPL39) and myeloid leukemia factor 2 (MLF2), by selective shRNA knockdown of genes from this tumorigenic signature, that impact breast cancer stem cell self-renewal and lung metastases. Analysis of 53 patient lung metastases confirmed damaging mutations in RPL39 and MLF2 in a significant number of samples, which conferred a gain-of-function phenotype. These mutations were statistically associated with shorter median time to distant relapse. We further describe a common mechanism of action through nitric oxide synthase signaling that is regulated by hypoxia.

Results

Identification of siRNA Targets for Breast Cancer Stem Cells. As described in the Introduction, we have previously published a 477-gene tumorigenic signature of BCSC self-renewal derived from patient biopsies (22). An shRNA library encompassing all 477 genes with the 2–3 shRNAs per gene was created, as previously published (23, 24). Self-renewal capacity using the mammosphere forming efficiency (MSFE) was assayed, with an empty vector shRNA and gamma secretase inhibitor (GSI) against the Notch pathway as controls. Two triple negative breast cancer cell lines, SUM159 and BT549, were treated with pGIPZ lentiviral particles, with eight biologic replicates. The MSFE was analyzed using a Wilcoxon rank sum test with 20% threshold for a positive hit (Fig. 1*A*). The Notch pathway inhibitor GSI dramatically reduced mammosphere formation at 10 μM concentration (Fig. 1*B*). A short list of target genes was then defined using Z score analysis, showing reduced MSFE in both cell lines of all shRNAs in the screen (Fig. 1*C*). Only five

Significance

This manuscript describes the identification and characterization of two previously unidentified cancer genes, ribosomal protein L39 and myeloid leukemia factor 2, that play an important role in tumor initiation and metastasis. Knockdown of these genes in triple negative breast cancer (TNBC) models significantly reduces primary-tumor growth, as well as metastasis. Mutations in these genes are associated with worse survival in breast-cancer patients. Both genes are regulated by the nitric oxide signaling pathway. Identification of these two genes represents a significant breakthrough in our understanding of treatment resistance in TNBC. Targeting these genes could alter clinical practice for tumor metastasis in future and improve outcomes of patients with breast cancer.

Author contributions: B.D., S.G.-P., V.M., S.S.G., and J.C.C. designed research; B.D., S.G.-P., and X.C. performed research; K.-D.Y., Z.S., X. Li, M.G., Z.L., H.S., X. Liu, M.F., and M.K. contributed new reagents/analytic tools; B.D., S.G.-P., R.Z., S.B., S.R., P.S.-S., Y.C., T.H.-M.H., M.Z., and S.T.C.W. analyzed data; and B.D., S.G.-P., and J.C.C. wrote the paper.

The authors declare no conflict of interest.

*This Direct Submission article had a prearranged editor.

Freely available online through the PNAS open access option.

[1]B.D. and S.G.-P. contributed equally to this work.

[2]To whom correspondence should be addressed. E-mail: jcchang@houstonmethodist.org.

This article contains supporting information online at www.pnas.org/lookup/suppl/doi:10.1073/pnas.1320769111/-/DCSupplemental.

shRNAs showed significantly reduced expression in both SUM159 and BT549 cell lines ($P < 0.05$) (Fig. 1 *C* and *D*). The statistically significant genes were rescreened with multiplicity of infection of 10 for $n = 6$ replicates, using both SUM159 and BT4549 cell lines (Fig. 1*E*). Specifically, we chose the top two genes, RPL39 and MLF2, based on the effectiveness of down-regulation of BCSC renewal capacity by lentiviral shRNA knockdown of these two cell lines (SUM 159 and BT549) (Fig. S1). These top two genes, RPL39 and MLF2, were then selected for further study.

To develop potential therapeutics, we then identified the corresponding siRNA sequence for RPL39 and MLF2. We tested target engagement for three siRNA sequences per gene in vitro (Fig. S2) and selected the optimal siRNA sequence for further studies. We then tested the specificity of the optimal siRNA using knockdown followed by rescue and analysis by quantitative reverse transcriptase polymerase chain reaction (q-RT-PCR) and Western analysis (Fig. S3). The optimal siRNAs were found to significantly reduce MSFE in three cell lines (Fig. 1*F*).

In Vivo Xenograft Treatment Studies Show Significant Reduction in Tumor Volume and Improved Median Time to Survival with siRNAs Against RPL39 and MLF2. We initiated in vivo studies to measure the treatment efficacy of these siRNAs in MDAMB231 tumor xenografts. Significant reduction in tumor volume was observed in RPL39- and MLF2-treated groups, compared with vehicle-treated groups (Fig. 2*A*) ($P < 0.05$, Mann–Whitney rank sum test). Additionally, the combination of RPL39/ MLF2 siRNAs with chemotherapy further significantly reduced tumor volume compared with docetaxel chemotherapy alone (Fig. 2*B*) ($P < 0.05$, Mann–Whitney rank sum test).

Next, to assess whether the combination of siRNA/docetaxel could improve survival, treatment was aborted after two cycles, and time to survival was measured. Most importantly, the combination of RPL39 or MLF2 siRNA with chemotherapy significantly prolonged median survival over chemotherapy alone ($P < 0.05$, Mann–Whitney rank sum test). (Fig. 2*C*), mimicking the adjuvant setting in the treatment of early breast cancer with the maximum ability to impact survival in patients.

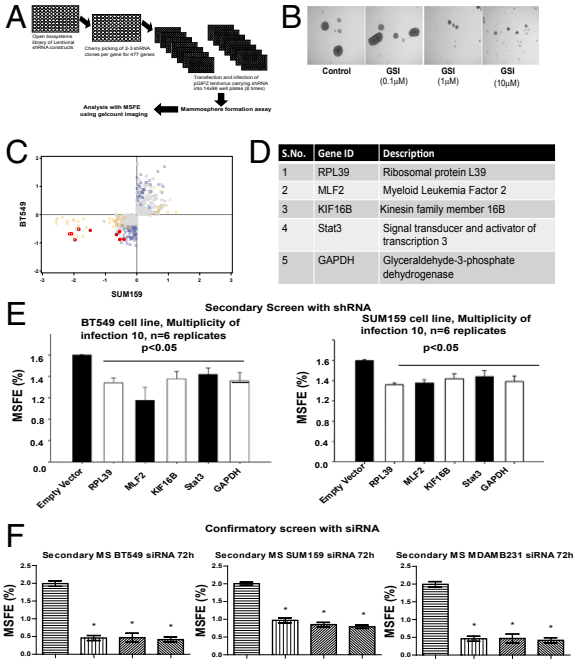

Fig. 1. Identification of siRNA targets. (*A*) Schematic representation of lentiviral screen for tumorigenic signature using the Open Biosystems GIPZ vector system. shRNAs targeting 477 genes along with controls were plated onto 14 × 96-well plates for a total of 1,128 shRNA in SUM159 and BT549 cell lines. (*B*) Increasing concentration of positive control Notch inhibitor (GSI) added to SUM159 cells to demonstrate a dose-dependent decrease in mammosphere forming efficiency. (*C*) Identification of top targets using Z score analysis of data in SUM19 and BT549 cell lines. Activity in both cell lines is color-coded, with bold red circles denoting reduced MSFE in both lines, and open red and gray circles denoting reduced MSFE in SUM159 and BT549, respectively; others are nonsignificant. (*D*) List of five genes identified by Z score analysis. (*E*) Validation of BCSC targets was conducted with a low titer of virus (pGIPZ vector) at a multiplicity of infection of 10 using MSFE. (*F*) Secondary MSFE with siRNA (50 nM) from the sequence derived from pGIPZ vector shRNA against MLF2 and RPL39 in three triple negative cell lines, MDAMB231, SUM159, and BT549. Data analyzed by one way ANOVA and plotted as mean + SEM for $n = 6$ replicates; $^*P < 0.05$.

In Vivo Studies Demonstrate the Effect on BCSCs and Lung Metastasis with siRNAs Against RPL39 and MLF2. We conducted a series of short-term studies to measure the effect of the siRNAs in a patient-derived human cancer triple negative breast cancer xenograft model (BCM2665) and further confirmed results in a second triple negative cell line model, SUM159. A multistage vector (MSV) liposomal nanoparticle delivery platform was used for sustained siRNA delivery with a single 2-wk dose (25). Significant reduction in tumor volume was observed in BCM2665 treated with RPL39 and MLF2 siRNA alone (Fig. 2*D*, *Left*) and with the combination of siRNA plus docetaxel vs. docetaxel (20 mg/kg) (Fig. 2*D*, *Right*). Similar results were obtained in SUM159 xenografts (Fig. S4). Significant reduction in secondary MSFE and nonsignificant decrease in Aldefluor due to the variability of marker with RPL39 and MLF2 siRNAs was observed (Fig. 2*E*). The Aldefluor assay was used to assess BCSCs because the BCM2665 patient-derived model system does not express $CD44^+/CD24^{low/-}$ cells (26). Statistically significant reduction of Aldefluor in SUM159 xenograft (Fig. S4) was observed. Additionally, target engagement was demonstrated by immunohistochemical analysis of RPL39 siRNA- and MLF2 siRNA-treated samples in BCM2665 (Fig. 2*F*) and SUM159 xenografts (Fig. S4).

In vivo limiting dilution assays (LDAs), which determine tumor initiating capacity, were conducted with tumors from SUM159 and MDAMB231 xenografts treated in vivo with RPL39 and MLF2 siRNA. SUM159 vehicle-treated group yielded 10/12 tumors, with a significant decrease in RPL39-treated (2/12) as well as MLF2-treated groups (4/12) ($P < 0.05$, Fisher's exact test) at 5 wk with 50,000 cells. Similarly, with MDAMB231 xenografts, the vehicle-treated group yielded 9/12 tumors, with a significant decrease in RPL39-treated (4/12) and MLF2-treated (2/12) xenografts (Fig. 2*G*). These data were confirmed with a patient-derived xenograft (BCM 2665). The vehicle group yielded 9/10 tumors with a significant decrease in RPL39-treated (1/10) as well as MLF2-treated (0/10) groups at 3.5 wk with 50,000 cells ($P < 0.05$, Fisher's exact test). Similar significant results were seen with 200,000 cells (Fig. 2*H*).

SCID-Beige mice were injected with luciferase-tagged MDAMB231 cells and treated with siRNA against RPL39 or MLF2 packaged in liposome nanoparticles twice weekly simultaneously, and then killed at week 6. A representative image of RPL39- and MLF2-treated mice 6 wk after primary-tumor injection is shown in Fig. 2*H*. All of the animals (12/12) treated with the scrambled siRNA group showed lung metastasis using in vivo International Veternary Information Service imaging whereas mice treated with RPL39 siRNA (5/11)and MLF2 siRNA (8/12) had significant reduction in lung metastasis (χ^2 test; RPL39, $P < 0.05$; MLF2, $P < 0.05$). Moreover, the luciferase analysis showed a significant reduction in the luminescence upon treatment with RPL39 and MLF2 siRNAs, respectively ($P < 0.05$) over time (Fig. 2*I*).

Increase in Cell Migration, MSFE, and Proliferation with RPL39 and MLF2 Overexpression. Overexpression of RPL39 and MLF2 in both MDAMB231 and BT549 cells significantly increased the wound-healing capacity with concomitant increase in migration index (Fig. 3*A*). Additionally, significant increase in secondary MSFE was observed, suggesting an important role for these genes in BCSC self-renewal (Fig. 3*B*). We also observed a significant increase in proliferation (Fig. 3*C*) with overexpression of RPL39 and MLF2. To demonstrate specificity of signaling by NOS pathway, rescue experiments were performed. RPL39 and MLF2 plasmids were able to reverse the siRNA-induced reduction in wound-healing capacity (Fig. S5 *A* and *B*).

CELL BIOLOGY

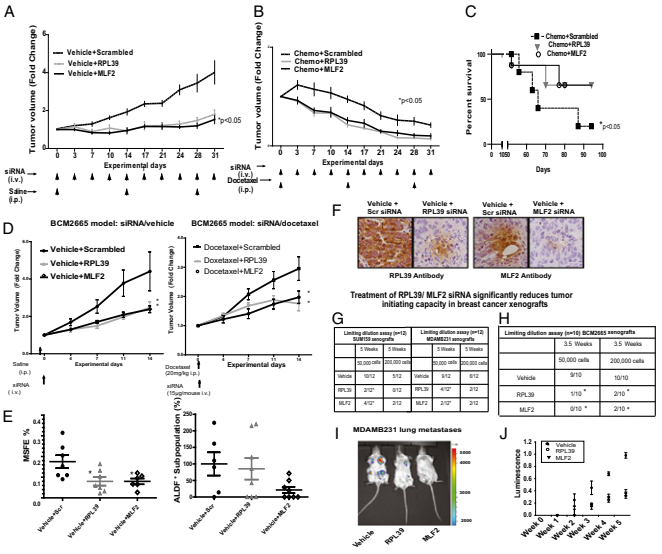

Fig. 2. In vivo treatment of primary cancer and lung metastasis xenografts with RPL39 and MLF2 siRNAs. Patient-derived tumor xenograft BCM2665 was transplanted, and MDAMB231 cell lines were injected into the mammary fat pad of SCID-Beige mice and randomized into six groups (n = 9 each): vehicle plus scrambled siRNA, vehicle plus RPL39 siRNA, vehicle plus MLF2 siRNA, docetaxel (20 mg/kg, i.p.) plus scrambled siRNA, docetaxel (20 mg/kg, i.p.) plus RPL39 siRNA, and docetaxel (20 mg/kg, i.p.) plus MLF2 siRNA. (*A*) Tumor volume fold change in MDAMB231 xenografts treated with scrambled, RPL39, and MLF2 siRNA respectively. (*B*) Tumor volume fold change in combination therapy with docetaxel plus siRNA (scrambled, RPL39, and MLF2) over three cycles. (*C*) Kaplan–Meier analysis of median survival of mice treated with docetaxel vs. combination therapy. (*D*) Tumor volume fold change in BCM2665 tumor-bearing animals treated with scrambled, RPL39, and MLF2 MSV siRNA alone and in combination with docetaxel. (*E*) Secondary MSFE was determined on day 28 and % ALDF$^+$ cells were determined using Aldefluor assay by flow cytometry. Data analyzed by one way ANOVA and plotted as mean + SEM for n = 9 replicates; *$P < 0.05$. (*F*) Target engagement for RPL39 and MLF2 is demonstrated in IHC sections stained for RPL39 and MLF2. (*G*) Limiting dilution assays in SUM159 and MDAMB231 xenografts were treated with siRNA against RPL39 and MLF2 (*$P < 0.05$, Fisher's exact test). (*H*) Limiting dilution assays using patient-derived xenograft BCM2665 treated with siRNA against RPL39 and MLF2 (*$P < 0.05$, Fisher's exact test). (*I*) Representative image of RPL39- and MLF2-treated mice 6 wk after primary-tumor injection. (*J*) Quantification of luminescence data demonstrates a significant reduction in luciferase activity upon RPL39 and MLF2 siRNA treatment.

RPL39 and MLF2 Affect Nitric Oxide Synthase and Hypoxia Signaling Pathway. Mutual-exclusivity analysis of RPL39 and MLF2 using The Cancer Genome Atlas (TCGA) breast cancer database determined that RPL39 and MLF2 co-occur at odds ratio of >10 (P = 0.02), suggesting a common mechanistic pathway (Fig. 4*A*) (27). Microarray analysis of siRNA-treated patient-derived human-cancer-in-mice xenograft BCM2665 was then performed to determine alterations in gene expression, followed by Ingenuity Pathway Analysis of the top signaling pathways common to both RPL39 and MLF2 siRNA-treated samples. Differential expression of "cellular effects of sildenafil (Viagra)" reflecting the nitric oxide signaling pathway (Fig. 4 *B* and *C* and Tables S1 and S2) was present for both RPL39 and MLF2. Thus, we specifically analyzed the nitric oxide synthases [inducible NOS (iNOS), endothelial NOS (eNOS), and neuronal NOS (nNOS)] and their impact on RPL39 and MLF2.

Overexpression of RPL39 and MLF2 led to an increase in eNOS and iNOS signaling with no change in nNOS in three cell lines (Fig. 4*D*). A clear reduction in iNOS signaling, together with decrease in eNOS without much change in nNOS, was observed with RPL39/MLF2 siRNA treatment (Fig. 4*E*). Next, rescue experiments were performed to test whether RPL39 and MLF2 were modulated in an NOS-dependent manner. These genes were overexpressed in two triple negative breast cancer cells lines, and NOS signaling was inhibited by NG-nitro-L-arginine methyl ester (L-NAME), a small-molecule inhibitor for NOS. Wound healing induced by RPL39 and MLF2 genes was significantly reduced in the presence of L-NAME (Fig. 4*F*), which was rescued using three molar excess of L-arginine, demonstrating a role of NOS signaling in both RPL39 and MLF2 (Fig. 4*F*). Additionally, we observed that the reduction in wound healing capacity caused by siRNA against iNOS could be directly rescued by either RPL39 or MLF2 plasmid (Fig. S5 *C* and *D*).

The relationship between nitric oxide synthase signaling and hypoxia has been well described in various tissue types (28–31). Hypoxia (1% O_2), in an HIF1α-dependent manner, induced RPL39 and MLF2 with concomitant increase in iNOS in two breast cancer cell lines (SUM159 and MDAMB231) (Fig. 5*A*). Inhibition of NO signaling by specific iNOS inhibitor 1400W decreased expression of RPL39 and MLF2 in an HIF1α-dependent manner in two cell lines (MDAMB231 and SUM159) (Fig. 5*B*). This inhibitor also decreased soluble guanylate cyclase (SCG) and cyclic-GMP dependent kinase-1 (PKG-1), which are directly downstream of NOS (Fig. 5*B*) whereas overexpression of RPL39 and MLF2 increased SGC and PKG-1, as expected in canonical iNOS-dependent signaling (Fig. 5*B*). Additionally, overexpression of RPL39/MLF2 genes, followed by hypoxic (1% O_2) conditions, dramatically reduced HIF1α expression (Fig. 5*C*), thus suggesting a potential feedback loop between HIF1α-dependent signaling and RPL39/MLF2 (Fig. 5*F*). We next tested the correlation between RPL39/MLF2 and HIF1α hypoxia-related signaling in siRNA-treated human xenograft (BCM2665) using gene specific enrichment analysis (GSEA) (32). Our results indicate a direct correlation between HIF1α-mediated hypoxia and RPL39/MLF2 (Fig. 5 *C* and *D*). The differential expression of five out of seven hypoxia-related genes (EIF1A1, ECE1, CAT, EPAS1, and SNRNP70) was confirmed by q-RT-PCR in patient-derived BCM2665 xenograft tumors (Fig. 5*E*).

Mutations in RPL39 and MLF2 Are Detected in Patient Breast Cancer Lung Metastasis. As described in the *Results* subsection on the in vivo studies of lung metastasis, a significant reduction in lung metastases effect with siRNAs against RPL39 and MLF2 was observed in vivo, suggesting a potential role of these genes in metastasis. Eight patient deidentified lung metastases were obtained and analyzed

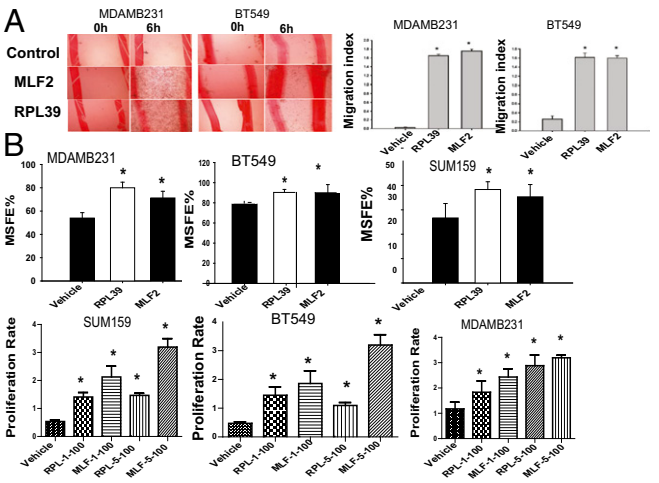

Fig. 3. Increase in wound healing, MSFE, and proliferation with RPL39 and MLF2 overexpression. (*A*) Representative image of MDAMB231 and BT549 cells treated with vehicle, RPL39, and MLF2. Overexpression of RPL39 and MLF2 genes demonstrates a statistically significant increase in the migration index of these cells. (*B*) The % secondary MSFE was determined with overexpression of RPL39 and MLF2 plasmid DNA in three triple negative breast cell lines, SUM159, BT549, and MDAMB231, in mammosphere growth media. Data were analyzed at 72 h. (*C*) A dose-dependent increase in proliferation was observed upon 1 μg and 5 μg of plasmid DNA transfection in the three breast cancer cell lines.

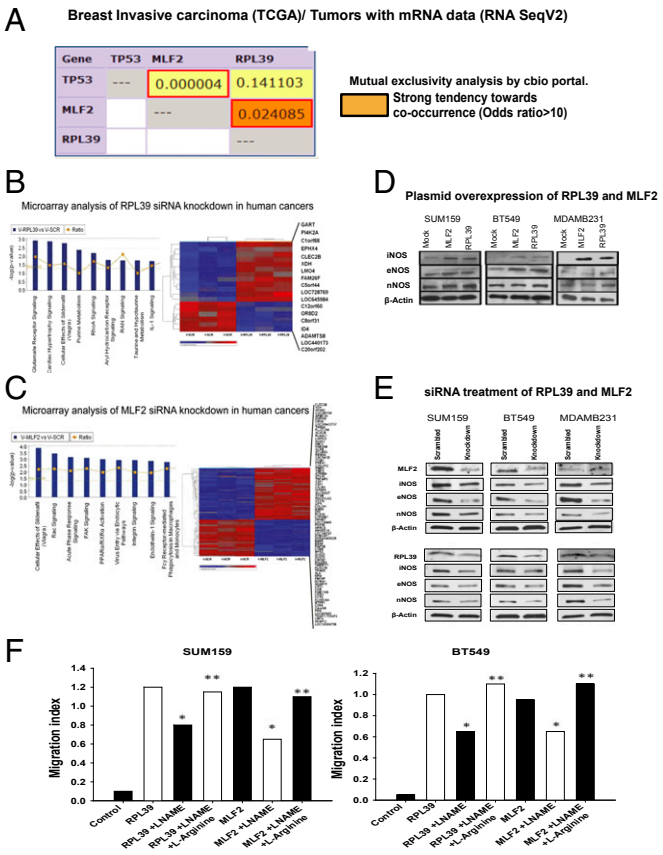

Fig. 4. RPL39 and MLF2 affect nitric oxide synthase (NOS) signaling. (*A*) Mutual exclusivity analysis of RPL39 and MLF2 in TCGA breast-cancer database demonstrates a statistically significant chance of co-occurrence odds ratio > 10 ($P = 0.02$). These data show strong tendency of co-occurrence for these two genes in breast cancer. (*B* and *C*) Microarray analysis of RPL39 and MLF2 siRNA, respectively, compared with scrambled siRNA in patient-derived xenografts BCM2665, at $P < 0.005$ and fold change >1.5. (*D*) Western analysis of control vs. overexpression of RPL39/ MLF2 shows an increase in both iNOS and eNOS with no changes in nNOS in two triple negative cell lines. (*E*) Western analysis of siRNA-treated samples comparing scrambled siRNA vs. MLF2/RPL39 siRNA, in vitro in three cell lines, SUM159, BT549, and MDAMB231, shows decrease in eNOS and iNOS, with no substantial change in nNOS. (*F*) Wound-healing assays were performed to confirm the role of NOS signaling in RPL39 and MLF2 overexpressing cell lines, using NOS inhibitor L-NAME. This inhibition was rescued by addition of three molar excess L-arginine.

for mutations in RPL39 and MLF2 gene using RNA deep sequencing. As shown in Fig. 6*A*, four damaging mutations were determined by SIFT (sorting intolerant from tolerant) analysis, two each in RPL39 (A14V and G50S) and MLF2 (D12H and R158W).

Next, we tested whether these mutations conferred a gain-of-function. Wild type RPL39 and MLF2 overexpression vs. mutations were incorporated in plasmids for RPL39 (A14V and G50S) and MLF2 (D12H and R158W) in two triple negative cell lines. Representative images for wild-type (black arrows) and mutant (red arrows) competitive allele-specific TaqMan (CAST) PCR assays (Life Technologies) are shown in Fig. 6*A*. Increases in wound-healing capacity were confirmed with three mutations, RPL39 (A14V) and MLF2 (D12H and R158W), over the wild-type plasmid in a 4-h time frame (Fig. 6*B* and Fig. S6).

Analyses of 477 primary breast cancers from The Cancer Genome Atlas (TCGA) CGHub (http://cghub.ucsc.edu) for mutations in either RPL39 or MLF2 were then conducted. Recently, mutation R158W in MLF2 was reported in non-small cell lung cancer (33), but not in breast cancer. We next tested the hypothesis of tumor heterogeneity within primary cancers and clonal selection with the small subpopulation of cells with stem-like properties showing increased metastatic propensity to the lung. Five matched primary and lung metastases were tested that were known to have mutations in RPL39 or MLF2 in lung metastases. Using CAST PCR (Life Technologies), no amplification was observed in all five individual primary tumors whereas mutations were identified in their matched lung metastatic pair. These data lend support to the observation that the frequency of the mutations may be too low in the primary tumors to be detected by conventional methods. Additionally, we tested these mutations by DNA-seq. Our results confirmed the lack of mutations in the primary samples, and 2/3 mutations were confirmed in the metastatic samples (Table S3) (34, 35). Competitive allele-specific PCR is a robust technology to detect mutations in formalin-fixed paraffin-embedded samples as shown in Fig. 6 (36–38).

Mutations in RPL39 (A14V) and MLF2 (D12H and R158W) Are Associated with Shorter Median Time to Relapse. In the clinical setting, resections of lung metastases are very rarely performed. We next examined mutations in RPL39 and MLF2 with competitive allele-specific PCR using genomic DNA derived from 53 patient lung metastases, with both estrogen receptor (ERα) positive and negative tumors. No significant difference in mutation frequency was observed according to steroid hormone receptor status (Fig. 6*C*). We found mutation in 6/53 patients in A14V, 4/53 patients in D12H, and 12/53 in R158W (Fig. 6*C*).

The time from initial diagnosis to lung metastasis was then assessed. Patients harboring gain-of-function mutations in RPL39 and MLF2 had a significantly shorter median time to relapse compared with those without mutations ($P = 0.0259$, χ^2 test) (Fig. 6*D*).

Discussion

Relapse of primary breast cancer at a metastatic site is the major cause of death in patients. In this present study, we report the discovery of two relatively novel cancer genes, RPL39 and MLF2, and describe their importance in tumor initiation and metastasis. Recently, functional evidence for the presence of cancer stem cells was confirmed in glioblastomas (GBMs), squamous skin tumors, and intestinal adenomas (10–12). To our knowledge, we were one of the first groups to describe that breast cancer stem

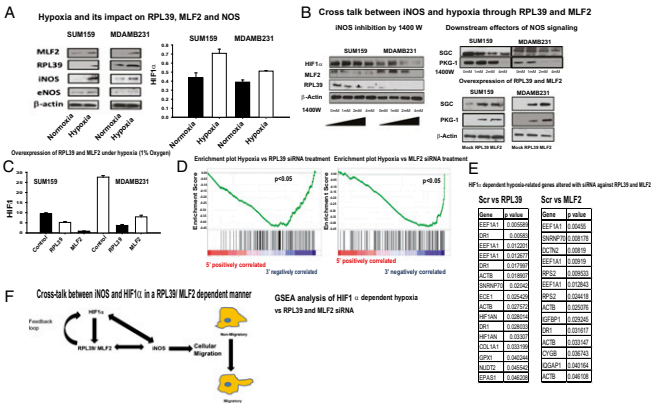

Fig. 5. RPL39 and MLF2 expression is altered by hypoxia. Two breast cancer cell lines (SUM159 and MDAMB231) were grown under hypoxic conditions (1% O_2) vs. normoxic conditions for 24 h. (*A*) These cell lines were analyzed for the two genes (MLF2 and RPL39), NOS signaling pathway (iNOS and eNOS) (*Right*). HIF1α levels were assessed by ELISA (*Left*). (*B*) Inhibition of iNOS under normoxia by 1400W reduced HIF1α, RPL39, and MLF2. Additionally, downstream effectors of NOS signaling SGC and PKG-1 were also reduced. Overexpression of RPL39 and MLF2 in these cell lines elevated SGC and PKG-1 levels. (*C*) RPL39 and MLF2 genes were overexpressed in SUM159 and MDAMB231 cells and exposed to hypoxia (1% O2) for 1 d followed by analysis of HIF1α levels by ELISA. (*D*) GSEA analysis of HIF1α-dependent hypoxia in patient-derived BCM2665 xenografts treated with siRNA against RPL39 and MLF2. (*E*) Tabular representation of HIF1α-dependent hypoxia-related genes that are significantly altered by siRNA against RPL39 and MLF2 from the same samples. (*F*) Diagram of cross-talk between iNOS, HIF1α, and RPL39/MLF2.

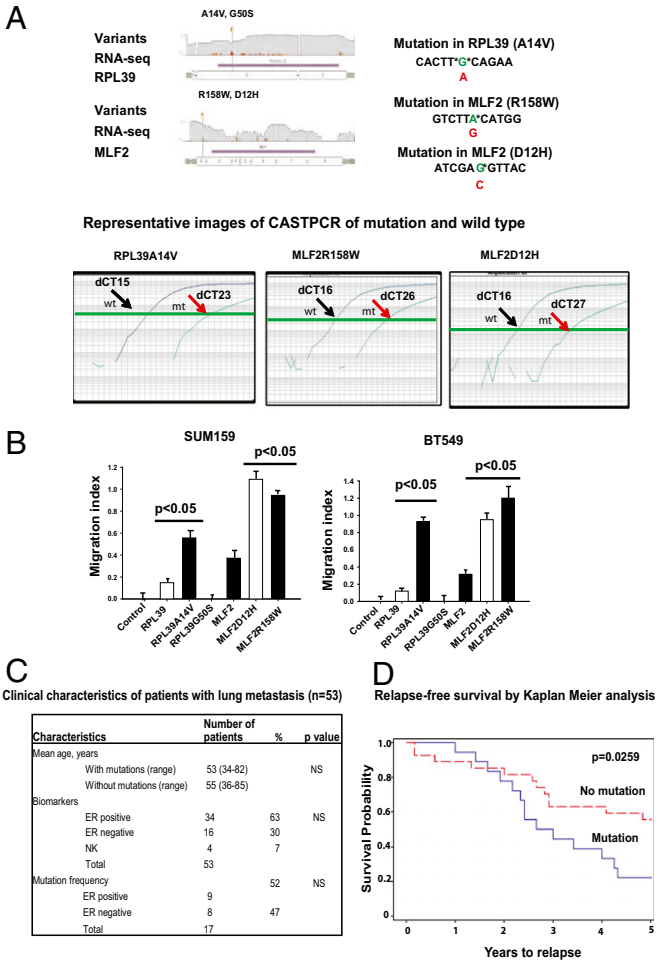

Characteristics	Number of patients	%	p value
Mean age, years			
With mutations (range)	53 (34-82)		NS
Without mutations (range)	55 (36-85)		
Biomarkers			
ER positive	34	63	NS
ER negative	16	30	
NK	4	7	
Total	53		
Mutation frequency		52	NS
ER positive	9		
ER negative	8	47	
Total	17		

Fig. 6. Identification and validation of damaging mutations in lung metastasis and sorted BCSC population. (*A*) Identification of mutations in RPL39 (A14V and G50S) and MLF2 (D12H and R158W) by RNA deep sequencing of patient lung metastases. Representative images of mutation detection CASTPCR assay results, showing wild-type (black arrows) and mutant (red arrows) curves in comparison. (*B*) The damaging mutations (RPL39_A14V, MLF2_D12H, and MLF2_R158W) confer a gain-of-function as demonstrated by increased wound-healing capacity posttransfection at 4 h. Data analyzed by one-way ANOVA and plotted as mean ± SEM for $n = 9$ replicates at $^*P < 0.005$. (*C*) Clinical characteristics of 53 patients with lung metastases and mutation status in RPL39 and MLF2. (*D*) Relapse-free survival in patients with lung metastases using Kaplan–Meier analysis.

cells demonstrate intrinsic resistance to conventional therapy in clinical samples (7, 22). Since these initial observations, other groups have confirmed these findings following conventional chemotherapy or radiation therapy (39). Metaanalyses of over 2,000 breast-cancer patients indicate that an increase in BCSC markers is significantly associated with an approximately threefold higher likelihood of metastases (5, 39).

In the present study, we used a functional approach to identify previously unidentified targets for cancer stem cells. We previously isolated BCSCs by isolating $CD44^+/CD24^{low/-}$ MS-forming cells from patient biopsies, and a tumorigenic signature of 477 genes (22). shRNA knockdown followed by a confirmatory screen yielded two top candidates, RPL39 and MLF2. RPL39 has been described as component of the 60S ribosomal complex located on chromosome X (XQ24), with a proposed role in spermatogenesis and translation (40, 41). MLF2 is located on chromosome 12 and may participate in chromosomal aberrations and defense response (42). RPL39 may play a role in ribosome biogenesis, which has been implicated in tumor growth progression and transformation (43, 44). Although almost nothing is known about the role of RPL39 in cancer, there is limited information available on MLF2. A series of amino acid modifications of MLF2 on Ser-144, -152, and -238 (45-47) and a somatic mutation (p.Phe80Cys) have been described in colorectal cancer (48).

Therapeutically, siRNAs are more desirable than lentiviral shRNA. Using the sequences derived from shRNA screening, we designed siRNAs against the top two targets, RPL39 and MLF2. We demonstrated a significant tumor reduction in patient-derived human cancer xenograft tumors treated with siRNAs against RPL39/MLF2 alone, as well as in combination with chemotherapy. More importantly, we found a significant benefit in prolonging median survival in the mice treated with a combination of chemotherapy and siRNA against RPL39/MLF2 compared with mice treated with chemotherapy alone. These siRNAs were effective in reducing cancer stem cells as defined by a reduction in MSFE, flow cytometry, and in limiting dilution assays. In these models, a profound impact on lung metastases with silencing RPL39 and MLF2 was observed, thus confirming the relevance of RPL39 and MLF2 in both tumor initiation and lung metastases.

Mutual exclusivity analysis using the TCGA database shared a highly statistically significant correlation between RPL39 and MLF2, suggesting a common mechanistic pathway. By Ingenuity Pathway Analysis, nitric oxide signaling was the top common pathway involved in the regulation of RPL39 and MLF2. Overexpression and knockdown of RPL39 and MLF2 demonstrated a concomitant change in iNOS. Importantly, nitric oxide synthase signaling, in particular iNOS, has been shown to play an important role in cancer stem cells and in other solid cancers like glioblastoma multiforme (49). Increased iNOS production has been shown to predict poor survival in breast-cancer patients (50). This study supports these previously published observations. A better understanding of the role of NO signaling in tumor tissues and stroma is essential to successfully target this pathway.

A relationship between NO signaling and hypoxia has been well-described (28–31). Cancer stem cells have been described to reside near hypoxic regions in solid cancers (19–21). Hypoxia transcriptionally activates iNOS in an HIF1α-dependent manner and promotes metastases primarily through HIF1α (30), which has been shown to regulate CD44 and its variants CD44v6, CD44v8, known markers of BCSCs (31). In our study, hypoxia (1% O_2) mediated by HIF1α increased iNOS signaling, along with induction of RPL39 and MLF2. Inhibition of iNOS by 1400W, a specific inhibitor of iNOS, reduced RPL39 and MLF2 in a dose-dependent manner. Additionally, HIF1α was concomitantly reduced, suggesting cross-talk between iNOS and HIF1α that is modulated by RPL39 and MLF2. An opposite effect was observed when RPL39 and MLF2 were overexpressed with an increase in the downstream effectors of NOS signaling pathway, SGC and PKG-1. These data suggest that RPL39 and MLF2 play a critical role in the cross-talk between iNOS and HIF1α. Under hypoxic conditions (1% oxygen), overexpression of RPL39 and MLF2 led to a reduction in HIF1α, suggesting a role for RPL39 and MLF2 as a negative feedback mechanism in HIF1α signaling. Other groups have described hypoxia and the regulation of CSC self-renewal. Our data support the results from these seminal papers (51–54).

Interestingly, bulk primary tumors from The Cancer Genome Atlas did not describe these mutations in breast cancer. These mutations may be present in a small subpopulation of cells and may not be detected due to the depth of coverage. A 100- to 1,000-fold coverage is required to detect clinically relevant somatic mutations in small tumor subpopulations because primary tumors are heterogeneous and this intratumoral heterogeneity may prevent the identification of specific mutations in distinct subpopulations (1, 55).

The gain-of-function mutations in RPL39 (AV14) and MLF2 (R158W and D12H) were present in a significant percentage of the lung metastases from 53 patients with both ERα-positive and ERα-negative tumors, suggesting that BCSCs with these mutations may be capable of multilineage differentiation (56). Importantly, the presence of these mutations was significantly associated with worse relapse-free survival and a shorter median time to relapse.

In conclusion, we have identified two relatively novel genes, RPL39 and MLF2, that affect cells with tumor-initiating properties,

as well as lung metastasis. We provide evidence that suggests that RPL39 and MLF2 affect nitric oxide synthase signaling and are altered by hypoxia. The role of the tumor microenvironment, specifically the interplay between hypoxia and nitric oxide synthase in breast-cancer initiation and metastasis, should be further studied.

Materials and Methods

Detailed methods on shRNA knockdown screen, mammosphere formation assays, siRNA packaging methods, in vitro proliferation, and wound healing assays are provided in *SI Materials and Methods*. Additionally, design of in vivo xenograft experiments, FACS analysis for BCSCs, Western blot analysis, immunohistochemistry, gene expression analysis, RNA-deep sequencing, SIFT mutational analysis, and confirmation of mutations by CAST PCR along with statistical methods can be found in the *SI Materials and Methods*. The animal experiments were approved by the Institutional Animal Care and Use Committee at the Houston Methodist Research Institute. The patient tissues were collected from the Houston Methodist Research Institute Biorepository approved by the Institutional Review Board. A prior informed consent was obtained.

ACKNOWLEDGMENTS. We thank Dr. Neal Copeland [National Academy of Sciences (NAS)] and Dr. Nancy Jenkins (NAS) (Directors of the Cancer Biology Program, Methodist Cancer Center) and Dr. Lewis Cantley (NAS) (Director of the Cancer Center, Weill Cornell Medical College) for their scientific input in designing the confirmation studies for RPL39 and MLF2 mutations and the mutual exclusivity analysis. We also thank Dr. Dan Liu at the Baylor College of Medicine Cell Based Assay Screening Service Core for assistance with shRNA screening. This work was supported by National Institutes of Health (NIH)/National Cancer Institute (NCI) Grants R01 CA138197 (to J.C.C.) and U54 CA149196 (to S.T.C.W.), Golfers Against Cancer (J.C.C.), the Breast Cancer Research Foundation (J.C.C.), Causes for a Cure (J.C.C.), Team Tiara (J.C.C.), the Emily W. Herrman Cancer Research Laboratory (J.C.C.), Komen for Cure KG 081694 (to J.C.C.), and Fundacion Alfonso Martin Escudero (S.G.-P.). Partial funds were acquired from the Ernest Cockrell Jr. Distinguished Endowed Chair (M.F.), US Department of Defense Grants W81XWH-09-1-0212 (to M.F.) and W81XWH-12-1-0414 (to M.F.), and the John S. Dunn Research Foundation (S.T.C.W.).

1. Gerlinger M, et al. (2012) Intratumor heterogeneity and branched evolution revealed by multiregion sequencing. *N Engl J Med* 366(10):883–892.
2. Campbell PJ, et al. (2010) The patterns and dynamics of genomic instability in metastatic pancreatic cancer. *Nature* 467(7319):1109–1113.
3. Campbell PJ, et al. (2008) Identification of somatically acquired rearrangements in cancer using genome-wide massively parallel paired-end sequencing. *Nat Genet* 40(6):722–729.
4. Shah NP, et al. (2002) Multiple BCR-ABL kinase domain mutations confer polyclonal resistance to the tyrosine kinase inhibitor imatinib (STI571) in chronic phase and blast crisis chronic myeloid leukemia. *Cancer Cell* 2(2):117–125.
5. Al-Hajj M, Wicha MS, Benito-Hernandez A, Morrison SJ, Clarke MF (2003) Prospective identification of tumorigenic breast cancer cells. *Proc Natl Acad Sci USA* 100(7):3983–3988.
6. Lapidot T, et al. (1994) A cell initiating human acute myeloid leukaemia after transplantation into SCID mice. *Nature* 367(6464):645–648.
7. Li X, et al. (2008) Intrinsic resistance of tumorigenic breast cancer cells to chemotherapy. *J Natl Cancer Inst* 100(9):672–679.
8. Smalley M, Ashworth A (2003) Stem cells and breast cancer: A field in transit. *Nat Rev Cancer* 3(11):832–844.
9. Stingl J, Caldas C (2007) Molecular heterogeneity of breast carcinomas and the cancer stem cell hypothesis. *Nat Rev Cancer* 7(10):791–799.
10. Chen J, et al. (2012) A restricted cell population propagates glioblastoma growth after chemotherapy. *Nature* 488(7412):522–526.
11. Driessens G, Beck B, Caauwe A, Simons BD, Blanpain C (2012) Defining the mode of tumour growth by clonal analysis. *Nature* 488(7412):527–530.
12. Schepers AG, et al. (2012) Lineage tracing reveals Lgr5+ stem cell activity in mouse intestinal adenomas. *Science* 337(6095):730–735.
13. Creighton CJ, Chang JC, Rosen JM (2010) Epithelial-mesenchymal transition (EMT) in tumor-initiating cells and its clinical implications in breast cancer. *J Mammary Gland Biol Neoplasia* 15(2):253–260.
14. Jones RJ, Matsui WH, Smith BD (2004) Cancer stem cells: Are we missing the target? *J Natl Cancer Inst* 96(8):583–585.
15. Brizel DM, Sibley GS, Prosnitz LR, Scher RL, Dewhirst MW (1997) Tumor hypoxia adversely affects the prognosis of carcinoma of the head and neck. *Int J Radiat Oncol Biol Phys* 38(2):285–289.
16. Hockel M, et al. (1996) Association between tumor hypoxia and malignant progression in advanced cancer of the uterine cervix. *Cancer Res* 56(19):4509–4515.
17. Nordsmark M, Overgaard M, Overgaard J (1996) Pretreatment oxygenation predicts radiation response in advanced squamous cell carcinoma of the head and neck. *Radiother Oncol* 41(1):31–39.
18. Sundfør K, Lyng H, Rofstad EK (1998) Tumour hypoxia and vascular density as predictors of metastasis in squamous cell carcinoma of the uterine cervix. *Br J Cancer* 78(6):822–827.
19. Li Z, et al. (2009) Hypoxia-inducible factors regulate tumorigenic capacity of glioma stem cells. *Cancer Cell* 15(6):501–513.
20. Jensen RL (2009) Brain tumor hypoxia: Tumorigenesis, angiogenesis, imaging, pseudoprogression, and as a therapeutic target. *J Neurooncol* 92(3):317–335.
21. Heddleston JM, et al. (2011) Glioma stem cell maintenance: The role of the microenvironment. *Curr Pharm Des* 17(23):2386–2401.
22. Creighton CJ, et al. (2009) Residual breast cancers after conventional therapy display mesenchymal as well as tumor-initiating features. *Proc Natl Acad Sci USA* 106(33):13820–13825.
23. Gobeil S, Zhu X, Doillon CJ, Green MR (2008) A genome-wide shRNA screen identifies GAS1 as a novel melanoma metastasis suppressor gene. *Genes Dev* 22(21):2932–2940.
24. Kessler JD, et al. (2012) A SUMOylation-dependent transcriptional subprogram is required for Myc-driven tumorigenesis. *Science* 335(6066):348–353.
25. Tasciotti E, Sakamoto J, Ferrari M (2009) Conference scene: Nanotechnology and medicine: The next big thing is really small. *Nanomedicine (Lond)* 4(6):619–621.
26. Landis MD, Lehmann BD, Pietenpol JA, Chang JC (2013) Patient-derived breast tumor xenografts facilitating personalized cancer therapy. *Breast Cancer Res* 15(1):201.
27. Cerami E, et al. (2012) The cBio cancer genomics portal: An open platform for exploring multidimensional cancer genomics data. *Cancer Discov* 2(5):401–404.
28. Matthews NE, Adams MA, Maxwell LR, Gofton TE, Graham CH (2001) Nitric oxide-mediated regulation of chemosensitivity in cancer cells. *J Natl Cancer Inst* 93(24):1879–1885.
29. Giordano FJ (2005) Oxygen, oxidative stress, hypoxia, and heart failure. *J Clin Invest* 115(3):500–508.
30. Liao D, Corle C, Seagroves TN, Johnson RS (2007) Hypoxia-inducible factor-1alpha is a key regulator of metastasis in a transgenic model of cancer initiation and progression. *Cancer Res* 67(2):563–572.
31. Krishnamachary B, et al. (2012) Hypoxia regulates CD44 and its variant isoforms through HIF-1α in triple negative breast cancer. *PLoS ONE* 7(8):e44078.
32. Subramanian A, et al. (2005) Gene set enrichment analysis: A knowledge-based approach for interpreting genome-wide expression profiles. *Proc Natl Acad Sci USA* 102(43):15545–15550.
33. Peifer M, et al. (2012) Integrative genome analyses identify key somatic driver mutations of small-cell lung cancer. *Nat Genet* 44(10):1104–1110.
34. Li H, Durbin R (2009) Fast and accurate short read alignment with Burrows-Wheeler transform. *Bioinformatics* 25(14):1754–1760.
35. Koboldt DC, et al. (2012) VarScan 2: Somatic mutation and copy number alteration discovery in cancer by exome sequencing. *Genome Res* 22(3):568–576.
36. Roma C, et al. (2013) Detection of EGFR mutations by TaqMan mutation detection assays powered by competitive allele-specific TaqMan PCR technology. *Biomed Res Int* 2013:385087.
37. Richter A, et al. (2013) A multisite blinded study for the detection of BRAF mutations in formalin-fixed, paraffin-embedded malignant melanoma. *Sci Rep* 3:1659.
38. Didelot A, et al. (2012) Competitive allele specific TaqMan PCR for KRAS, BRAF and EGFR mutation detection in clinical formalin fixed paraffin embedded samples. *Exp Mol Pathol* 92(3):275–280.
39. Lee A, et al. (2011) Chemotherapy response assay test and prognosis for breast cancer patients who have undergone anthracycline- and taxane-based chemotherapy. *J Breast Cancer* 14(4):283–288.
40. Uechi T, Tanaka T, Kenmochi N (2001) A complete map of the human ribosomal protein genes: Assignment of 80 genes to the cytogenetic map and implications for human disorders. *Genomics* 72(3):223–230.
41. Nadano D, Notsu T, Matsuda T, Sato T (2002) A human gene encoding a protein homologous to ribosomal protein L39 is normally expressed in the testis and derepressed in multiple cancer cells. *Biochim Biophys Acta* 1577(3):430–436.
42. Kuefer MU, et al. (1996) cDNA cloning, tissue distribution, and chromosomal localization of myelodysplasia/myeloid leukemia factor 2 (MLF2). *Genomics* 35(2):392–396.
43. Gandin V, et al. (2008) Eukaryotic initiation factor 6 is rate-limiting in translation, growth and transformation. *Nature* 455(7213):684–688.
44. Ray S, et al. (2013) Androgens and estrogens stimulate ribosome biogenesis in prostate and breast cancer cells in receptor dependent manner. *Gene* 526(1):46–53.
45. Molina H, Horn DM, Tang N, Mathivanan S, Pandey A (2007) Global proteomic profiling of phosphopeptides using electron transfer dissociation tandem mass spectrometry. *Proc Natl Acad Sci USA* 104(7):2199–2204.
46. Nousiainen M, Silljé HH, Sauer G, Nigg EA, Körner R (2006) Phosphoproteome analysis of the human mitotic spindle. *Proc Natl Acad Sci USA* 103(14):5391–5396.
47. Daub H, et al. (2008) Kinase-selective enrichment enables quantitative phosphoproteomics of the kinome across the cell cycle. *Mol Cell* 31(3):438–448.
48. Sjoblom T, et al. (2006) The consensus coding sequences of human breast and colorectal cancers. *Science* 314(5797):268–274.
49. Eyler CE, et al. (2011) Glioma stem cell proliferation and tumor growth are promoted by nitric oxide synthase-2. *Cell* 146(1):53–66.
50. Glynn SA, et al. (2010) Increased NOS2 predicts poor survival in estrogen receptor-negative breast cancer patients. *J Clin Invest* 120(11):3843–3854.
51. Heddleston JM, et al. (2012) Hypoxia-induced mixed-lineage leukemia 1 regulates glioma stem cell tumorigenic potential. *Cell Death Differ* 19(3):428–439.
52. Mathieu J, et al. (2011) HIF induces human embryonic stem cell markers in cancer cells. *Cancer Res* 71(13):4640–4652.
53. Heddleston JM, et al. (2010) Hypoxia inducible factors in cancer stem cells. *Br J Cancer* 102(5):789–795.
54. Dong C, et al. (2013) Loss of FBP1 by Snail-mediated repression provides metabolic advantages in basal-like breast cancer. *Cancer Cell* 23(3):316–331.
55. Burrell RA, McGranahan N, Bartek J, Swanton C (2013) The causes and consequences of genetic heterogeneity in cancer evolution. *Nature* 501(7467):338–345.
56. Visvader JE (2011) Cells of origin in cancer. *Nature* 469(7330):314–322.